

# EFFECTS OF STRONG MAGNETIC FIELDS IN NEUTRON STAR AND GRAVITATIONAL WAVE EMISSION

G. F. MARRANGHELLO

*Instituto de Física, Universidade Federal do Rio Grande do Sul  
91501-970 Porto Alegre, Brazil  
gfm@if.ufrgs.br*

We review in this work the properties of the nuclear and quark matter equations of state under the influence of a strong magnetic field, in special, its effects in the hadron-quark phase transition and in the global properties of compact stars. We describe moreover the emission of gravitational waves from a compact stars that goes over a hadron-quark phase transition in its inner core.

## 1 Introduction

In the last few years, the determination of properties of the equation of state (EoS) of nuclear matter has become one of the main goals in nuclear physics. Astrophysical observations together with the investigation of dense hadronic matter via high-energy colliders, BNL-RHIC and CERN-LHC, have brought excellent expectations on this matter.

Additionally, through the determination of masses and radii of neutron stars, one may establish important constrains in the parameters of nuclear models. For instance, Chandra X-Ray Observatory and BeppoSax are performing important analysis on neutron stars and pulsars X-Ray or thermal emission. Specially important are the new data about the masses of neutron stars, extracted from quasi-periodic oscillations (QPO) in low mass X-ray binaries (LMXB), specially the system of Vela X-1 pulsar; these data have given new information about the nuclear matter equation of state. Although most of the pulsar masses are found around the value of the Hulse and Taylor pulsar ( $1.44M_{\odot}$ ), the Vela X-1 pulsar has an inferred mass about  $1.86\pm 0.16M_{\odot}$ . This result indicates new relevant characteristics about the stiffness of the theoretical EoS. In addition, one must also mention the recent results obtained from the system RXJ 1856.5-3754, which shows special features concerning its temperature and evolution, leading to the conclusion, despite some still open questions, that it may be formed by extremely compacted strange quark matter ( $M\approx 1M_{\odot}$  and  $R\approx 6km$ ).

New important results from the research on gravitational waves are expected. For instance, we mention the detection of gravitational waves gener-

ated by rotating pulsars, phase-transitions, star-quakes or micro-collapses on neutron stars.

Very important aspect related to the structure of the EoS in neutron stars are the influence of a strong magnetic field in global static properties of the star and in particular its effects in the phase transition of hadron matter to a plasma of quarks and gluons inside the star.

In the following we briefly discuss these topics. We use, for the hadron phase, a modified version of the quantum hadrodynamics (QHD)<sup>1</sup> model and for the quark-gluon phase the MIT<sup>2</sup> bag model.

## 2 Nuclear Matter Equation of State

One consistent approach to describe nuclear matter is the pioneering work of Walecka which is based on effective field theory. Further developments were done by many authors from whose we extract the works by Boguta and Bodmer<sup>3</sup>, Zimanyi and Moszkowski<sup>4</sup> and Taurines et. al.<sup>5</sup>, developed in the following years.

We have used as the starting point of our study the lagrangian density

$$\begin{aligned}
\mathcal{L} = & \sum_B \bar{\psi}_B [i\gamma_\mu (\partial^\mu - g_{\omega B} \omega^\mu) - (M_B - g_\sigma \sigma)] \psi_B \\
& - \sum_B \bar{\psi}_B \left[ \frac{1}{2} g_\rho \boldsymbol{\tau} \cdot \boldsymbol{\rho}^\mu \right] \psi_B + \frac{bM}{3} \sigma^3 + \frac{c}{4} \sigma^4 \\
& + \frac{1}{2} (\partial_\mu \sigma \partial^\mu \sigma - m_\sigma^2 \sigma^2) - \frac{1}{4} \omega_{\mu\nu} \omega^{\mu\nu} + \frac{1}{2} m_\omega^2 \omega_\mu \omega^\mu \\
& - \frac{1}{4} \boldsymbol{\rho}_{\mu\nu} \cdot \boldsymbol{\rho}^{\mu\nu} + \frac{1}{2} m_\rho^2 \boldsymbol{\rho}_\mu \cdot \boldsymbol{\rho}^\mu + \sum_l \bar{\psi}_l [i\gamma_\mu \partial^\mu - M_l] \psi_l, \quad (1)
\end{aligned}$$

which includes the fundamental baryon octet (p, n,  $\Lambda$ ,  $\Sigma^+$ ,  $\Sigma^0$ ,  $\Sigma^-$ ,  $\Xi^-$ ,  $\Xi^0$ ) coupled to three mesons ( $\sigma$ ,  $\omega$ ,  $\rho$ ), and two free leptons ( $e$ ,  $\mu$ ). The scalar and vector coupling constants,  $g_\sigma$ ,  $g_\omega$  and the coefficients b, c are determined by fitting nuclear matter bulk properties, i. e., the binding energy  $E_b$  ( $= -16.3$  MeV), the compression modulus K ( $= 240$  MeV) and the effective nucleon mass  $M^* = M - g_\sigma \bar{\sigma}$  ( $= 732$  MeV) at saturation density  $\rho_0$  ( $= 0.153$  fm<sup>-3</sup>). The  $\rho$ -baryon coupling constant,  $g_\rho$ , is determined by fitting the nuclear matter asymmetry coefficient,  $a_4$  ( $= 32.5$  MeV) (for details see Refs.<sup>6,7</sup>).

Applying standard technics of field theory and solving the dynamical field equations at a mean-field level, one can extract expressions for the thermo-

dynamical quantities like pressure,  $p$ , and energy density,  $\epsilon$ , and verify the suitability of the model. The predictions for the experimental values of compression modulus,  $K$  and effective nucleon mass,  $M^*$ , result in excellent agreement with the experimental values for neutron star masses and radii<sup>6,8</sup>. In Fig. 1 we describe in particular the behavior of the distribution of species as a function of the total baryon density.

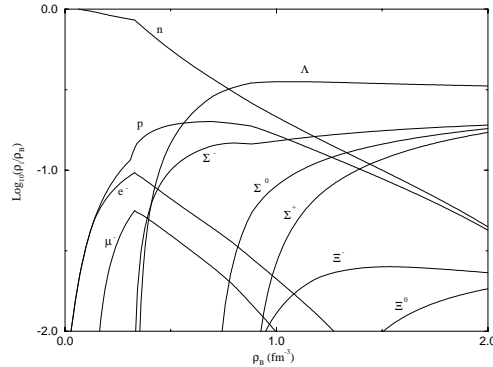


Figure 1. Particle distribution as function of baryon density.

### 3 Phase Transition to Quark Matter

The phase transition from nuclear to quark matter is expected to occur at high densities and/or high temperatures, and to restore chiral symmetry. We follow in this section the work of Heiselberg and Hjorth-Jensen<sup>9</sup> which describes the conditions for the occurrence of a mixed phase composed by hadrons and deconfined quarks. The occurrence of a mixed phase, first claimed by Glendenning<sup>10</sup>, where quark structures are immersed into a hadron matter (or vice-versa at higher densities), is now uncertain. This work will not clarify this topic, once it is model-dependent; however, as an application of this study we intend to propose possible differences on the detection of such phases inside hybrid stars.

Generally speaking, the physical properties of the transitions with one or more than one conserved charges are quite different. The most important feature is that the pressure may be constant or vary continuously with the proportion of phases in equilibrium. Reviewing Heiselberg's work, one can search for the answer respect to which kind of transition is energetically favored through an analysis of the bulk energy gained in such a transition and

the Coulomb and the surface energy relations, as stressed below.

Using the MIT bag model in the description of quark matter and combining the MIT expression for the thermodynamical potential

$$\begin{aligned} \Omega = & \sum_{q=u,d,s} \frac{-1}{4\pi^2} \left[ \mu_q k_{Fq} (\mu_q^2 - \frac{5}{2} m_q^2) + \frac{3}{2} m_q^4 \ln \left( \frac{\mu_q + k_{Fq}}{m_q} \right) \right] \\ & + \frac{2\alpha_c}{4\pi^3} \left[ 3 \left[ \mu_q k_{Fq} - m_q^2 - m_q^2 \ln \left( \frac{\mu_q + k_{Fq}}{m_q} \right) \right]^2 - 2k_{Fq}^4 - 3m_q^4 \ln^2 \left( \frac{m_q}{\mu_q} \right) \right] \\ & \times \left[ 6 \ln \left( \frac{\rho_r}{\mu_q} \right) \left( \mu_q k_{Fq} m_q^2 - m_q^4 \ln \left( \frac{\mu_q + k_{Fq}}{m_q} \right) \right) \right] + B, \end{aligned} \quad (2)$$

with the corresponding results of the model described in Eq. (1), one can relate the resulting energy densities in order to calculate the bulk energy of hadron-quark matter. However, due to large uncertainties in the estimates of bulk and surface properties, one cannot claim that the droplet phase is favored or not, once it depends crucially on the nuclear and quark matter properties.

If droplet sizes and separations are small compared with the Debye screening length,  $\lambda_D$ ,

$$\frac{1}{\lambda_D^2} = 4\pi \sum_i Q_i^2 \left( \frac{\partial n_i}{\partial \mu_i} \right)_{n_j, j \neq i} \quad (3)$$

where  $n_i$ ,  $\mu_i$  and  $Q_i$  are the number density, chemical potential and charge of particle species  $i$ , the electron density will be uniform to a good approximation. Screening effects can be estimated: if the characteristic spatial scales of structures are less than about 10 fm for the nuclear phase, and less than about 5 fm for the quark phase, screening effects will be unimportant, and the electron density will be essentially uniform; in the opposite case, the total charge densities for bulk nuclear and quark matter will both vanish.

When quark matter occupies only a small fraction,

$$f = \frac{V_{QM}}{V_{QM} + V_{NM}} \quad (4)$$

of the total volume, quarks will form spherical droplets. The surface energy per droplet is given by  $\epsilon_S = \sigma 4\pi R^2$ , where  $\sigma$  is the surface tension, and the Coulomb energy is

$$\epsilon_C = \frac{16\pi^2}{15} (\rho_{QM} - \rho_{NM})^2 R^5. \quad (5)$$

Minimizing the energy density with respect to  $R$ , one obtains the usual result  $\epsilon_s = 2\epsilon_C$  and finds a droplet radius

$$R = \left( \frac{15}{8\pi} \frac{\sigma}{(\rho_{QM} - \rho_{NM})^2} \right)^2. \quad (6)$$

These results cannot be considered definitive before a high precise determination of the surface tension,  $\sigma$ , is performed. However, for  $\sigma \sim 70 - 100 MeV$ , a mixed phase is unfavored and the star will have a density discontinuity. The result is a larger radius to support the mixed phase. The behavior of the equation of state for the constant pressure phase transition to quark matter, determined through our models, is shown below in Fig. 2.

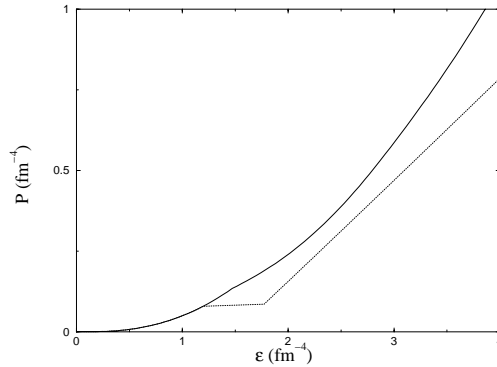


Figure 2. Equation of state for pure neutron star matter (solid line) and for the transition to quark matter (dotted line).

#### 4 Magnetic Field Effects

Several independent arguments link the class of *Soft  $\gamma$ -Ray Repeaters* (SGRs) and anomalous X-ray pulsars with neutron stars having ultra strong magnetic fields. In addition, two of four known SGRs directly imply, from their periods and spin-down rates, that the surface magnetic fields lay in the range  $(2 - 8) \times 10^{14} G$ . An estimate of the magnitude of the magnetic field strength needed to dramatically affect the neutron star structure yields  $B \sim 2 \times 10^{18} \frac{M/1.4M_{\odot}}{(R/10km)^2}$  in the interior of neutron stars<sup>11</sup>.

In this section we investigate the effects of very strong magnetic fields on the equation of state of dense matter with hyperons and quarks. In the presence of a magnetic field, the equation of state above nuclear saturation density

is significantly affected both by the Landau quantization and by magnetic moment interactions; this happens however only for fields strengths  $B > 10^{18}G$ .

The lagrangian density (Eq.1) can be re-written in order to include the magnetic field as

$$\begin{aligned}
\mathcal{L} = & \sum_B \bar{\psi}_B [i\gamma_\mu \partial^\mu - (M_B - g_{\sigma B}^* \sigma) - g_{\omega B}^* \gamma_\mu \omega^\mu + q_b \gamma_\mu A^\mu \\
& - \kappa_b \sigma_{\mu\nu} F^{\mu\nu}] \psi_B - \sum_B \psi_B [\frac{1}{2} g_{\varrho B}^* \gamma_\mu \boldsymbol{\tau} \cdot \boldsymbol{\varrho}^\mu] \psi_B \\
& + \sum_\lambda \bar{\psi}_\lambda [i\gamma_\mu \partial^\mu - m_\lambda + q_l \gamma_\mu A^\mu] \psi_\lambda \\
& + \frac{1}{2} (\partial_\mu \sigma \partial^\mu \sigma - m_\sigma^2 \sigma^2) - \frac{1}{4} \Omega_{\mu\nu} \Omega^{\mu\nu} - \frac{1}{4} F_{\mu\nu} F^{\mu\nu} \\
& + \frac{1}{2} m_\omega^2 \omega_\mu \omega^\mu - \frac{1}{4} \boldsymbol{\varrho}_{\mu\nu} \cdot \boldsymbol{\varrho}^{\mu\nu} + \frac{1}{2} m_\varrho^2 \boldsymbol{\varrho}_\mu \cdot \boldsymbol{\varrho}^\mu.
\end{aligned}$$

For detailed and well founded texts on magnetic field effects, we recommend Refs.<sup>12,13</sup>, from where one can find the energy spectrum for the protons given by

$$\begin{aligned}
E_p = & \sqrt{k_z^2 + \left( \sqrt{M_p^{*2} + 2 * (n + \frac{1}{2} + \frac{s}{2}) q_p B + s \kappa_p B} \right)^2} \\
& + g_\omega \omega_0 - \frac{1}{2} g_\varrho \varrho_0.
\end{aligned} \tag{7}$$

In a strong magnetic field, the particles motion are perpendicular to the field lines and are quantized having discrete *Landau orbitals*. The particles behave like a one-dimensional rather than a three-dimensional gas, and the stronger is the field, the smaller is the number of occupied *Landau levels*. Moreover, the energy of a charged particle changes significantly in the quantum limit if the magnetic field obeys  $H \geq H_c$ . With respect to the relativistic intensity of the effects, for electrons,  $H_c \sim 4 \times 10^{13}G$ , for  $u$  and  $d$  (massless quarks),  $H_c \sim 4 \times 10^{15}G$ , for  $s$ -quark,  $H_c \sim 10^{18}G$  and for protons,  $H_c \sim 10^{20}G$ .

Considering phase transition aspects, a strong magnetic field unfavour the mixed hadron-quark phase once it increases the electron number in the nuclear phase leaving the quark phase practically unchanged. This increases the droplet size as it was discussed in the previous section and in ref.<sup>14</sup>.

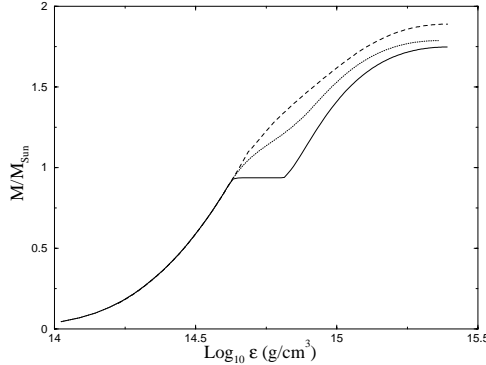


Figure 3. Masses of neutron star as a function of central energy density. The results for a hybrid star without mixed phase (solid line), with mixed phase (dotted line) and for a pure neutron star (dashed line) are presented.

## 5 Compact Stars

The first step through an analysis of compact stars recall the simpler solution of the general relativistic Einstein equations which represents a static and spherically symmetric star, the Schwarzschild solution, known as the Tolman-Oppenheimer-Volkoff (TOV) equations<sup>15,16</sup>. Thus, the TOV equations describe the structure of a static, spherical and isotropic star with the pressure  $p(r)$  and the energy density  $\epsilon(r)$  reflecting the underlying nuclear model. The TOV equations involve various constraints and boundary conditions: they must be evaluated for the initial condition  $\epsilon(0) = \epsilon_c$  (with  $\epsilon_c$  denoting the central density in the star) and  $M(0) = 0$  at  $r = 0$ ; the radius  $R$  of the star is determined under the condition that, on its surface, the pressure vanishes,  $p(r)|_{r=R} = 0$ .

The condition for chemical equilibrium for neutron stars are:

$$\mu_i = b_i \mu_n - q_i (\mu_\ell) \quad (8)$$

where  $\mu_i$  and  $\mu_\ell$  stand for the baryon and lepton chemical potentials, respectively;  $b_i$  is the baryon number and the baryon and lepton electrical charges are represented by  $q_i$ .

The corresponding equations for baryon number and electric charge conservation are:

$$\rho_{baryonic} = \sum_B \frac{k_{F,B}^3}{3\pi^2}, \quad (9)$$

and

$$\sum_B q_{e,B} \frac{k_{F,B}^3}{3\pi^2} - \sum_\ell \frac{k_{F,\ell}^3}{3\pi^2} = 0. \quad (10)$$

Here one can visualize the importance on the determination of the parameters of quark and nuclear matter, once they will reflect on the properties of compact stars. First, quark stars maximum mass,  $M$ , and radius,  $R$ , are directly governed, in conventional bag models, by the value of the bag constant ( $B_{60}$ ) as:

$$M = \frac{1.964M_\odot}{\sqrt{B_{60}}} ; R = \frac{10.71km}{\sqrt{B_{60}}} \quad (11)$$

where  $B_{60} = B/(60MeV/fm^3)$  in the massless quarks case. Additionally, the strong coupling constant  $\alpha_c$  is also related to quark star properties. Both  $B_{60}$  and  $\alpha_c$  will determine whether or not the hadron-quark phase transition will take place. The sequence of neutron stars (mass-energy density relation) and the behavior of the energy density in the interior of a neutron star is presented in the figures below.

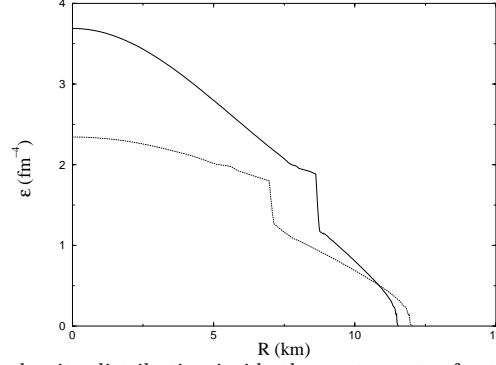


Figure 4. Energy density distribution inside the neutron star for two different central energies.

The nuclear matter coupling constants  $g_{B\sigma}$ ,  $g_{B\omega}$  and  $g_{B\rho}$  present the same sensibility and uncertainties. Nuclear matter properties of the nucleon effective mass, compression modulus of symmetric nuclear matter and particle distribution play also an important role on the phase transition and star properties and, consequently, on the emission of gravitational wave as we will discuss in the following sections.



The effects of the presence of a strong magnetic field are shown in the figures that describe the equation of state, Fig.5, neutron star masses, Fig.6, and particle distribution, Fig.7.

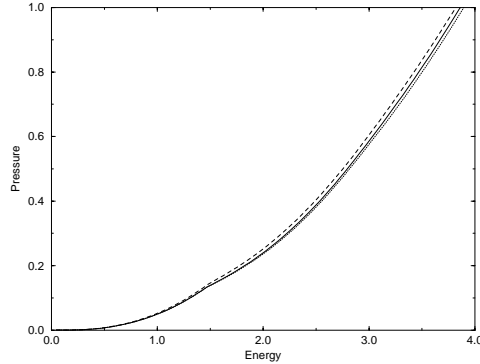


Figure 5. Equation of state for neutron star for  $B=0$  (solid line) and  $B=10^{18}\text{G}$  with (dotted line) and without (dashed line) the presence of the anomalous magnetic moment.

## 6 The Conversion of Neutron Stars to Hybrid Stars

The transition from the configuration of pure hyperon stars (H) to hybrid stars (HQ) may occur through the formation of a metastable core, built up by an increasing central density which may be a consequence of a continuous spin-down or other different mechanisms in the star. This transition releases energy, exciting mainly the radial modes of the star. These modes do not emit GWs, unless when coupled with rotation, a situation which will be assumed here.

Strange matter is assumed to be absolutely stable and a seed of strange matter in a neutron star would convert the star into a hybrid or strange star. The speed at which this conversion occurs was calculated by Olinto<sup>17</sup>, taking into account the rate at which the down- and strange-quark Fermi seas equilibrate via weak interactions and the diffusion of strange-quarks towards the conversion front.

Accordingly to Ref.<sup>17</sup>, cold neutron star matter can convert to strange star matter with speeds ranging from  $5\text{km/s}$  to  $2 \times 10^4\text{km/s}$ . The outcome of such an event would emit an incredible amount of energy from 0.5ms to 2s.

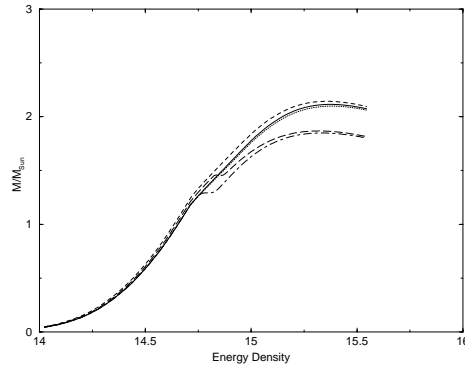


Figure 6. Masses of pure neutron star at  $B=0$  (solid line) and  $B=10^{18}\text{G}$  with (dotted line) and without (dashed line) the effects of anomalous magnetic moment and the masses of hybrid stars at  $B=10^{18}\text{G}$  (long dashed line) and  $B=5 \times 10^{18}\text{G}$  (dot-dashed line) as functions of the central energy density.

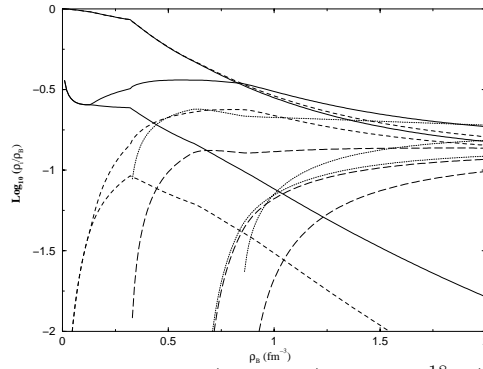


Figure 7. Particles distribution at  $B=0$  (solid lines) and  $B=10^{18}\text{G}$  (dotted line) as functions of the baryonic density.

We apply this discussion to the partial conversion of a neutron star to strange matter, forming a hybrid star.

However, the emission of gravitational waves, which will be discussed in the next section, can only *recognize* the phase transition after a structural rearrangement of the star, which shall reduce its radius and gravitational mass, conserving its total baryon number. Such mechanism has already been studied by Bombaci<sup>18</sup> for the emission of  $\gamma$ -ray bursts.

## 7 Gravitational Wave Emission

In order to simplify the analysis, I will consider that most of the mechanical energy of GW emission is in the fundamental mode. In this case, the gravitational strain amplitude can be written as

$$h(t) = h_0 e^{-(t/\tau_{gw} - i\omega_0 t)} \quad (12)$$

where  $h_0$  is the initial amplitude,  $\omega_0$  is the angular frequency of the mode and  $\tau_{gw}$  is the corresponding damping timescale. The initial amplitude is related to the total energy  $E_g$  dissipated as GWs according to the relation<sup>19</sup>

$$h_0 = \frac{4}{\omega_0 r} \left[ \frac{GE_g}{\tau_{gw} c^3} \right]^{1/2} \quad (13)$$

where  $G$  is the gravitational constant,  $c$  is the velocity of light and  $r$  is the distance to the source.

Relativistic calculations of radial oscillations of a neutron star with a quark core were recently performed by Sahu et al.<sup>20</sup>. However, the relativistic models computed by those authors do not have a surface of discontinuity where an energy jump occurs. Instead, a mixing region was considered, where the charges (electric and baryonic) are conserved globally but not locally<sup>10</sup>. Oscillations of star modes including an abrupt transition between the mantle and the core were considered in Refs.<sup>7,21,22</sup>. However, a Newtonian treatment was adopted and the equation of state used in the calculations does not correspond to any specific nuclear interaction model. In spite of these simplifications, these hybrid models suggest that a *rapid* phase transition occurs as the result from the formation of a pion condensate, then proceeds at the rate of strong interaction and affects substantially the mode frequencies. However, the situation is quite different for *slow* phase transitions (the present case), where the mode frequencies are quite similar to those of an *one-phase* star<sup>21</sup>. In this case, scaling the results of Ref.<sup>21</sup>, the frequency of the fundamental mode (uncorrected for gravitational redshift) is given approximately by

$$\nu_0 \approx 63.8 \left[ \frac{(M/M_\odot)}{R^3} \right]^{1/2} \text{ kHz} \quad (14)$$

where the mass is given in solar units and the radius in km.

Once the transition to quark-gluon matter occurs, the weak interaction processes for the quarks  $u$ ,  $d$  and  $s$

$$u + s \rightarrow d + u \quad \text{and} \quad d + u \rightarrow u + s \quad (15)$$

will take place. Since these reactions are relatively slow, they are not balanced while the oscillations last and thus, they dissipate mechanical energy into heat<sup>23</sup>. According to calculations of Ref.<sup>21</sup>, the dissipation time-scale can be estimated by the relation

$$\tau_d \approx 0.01 \left( \frac{150 \text{ MeV}}{m_s} \right)^4 \left( \frac{M_\odot}{M_c} \right) s \quad (16)$$

where  $m_s$  is the mass of the s-quark in MeV and  $M_c$  is the mass of the deconfined core in solar masses. This equation is valid for temperatures in the range  $10^8 - 10^9 K$ . On the other hand, the damping time-scale by GW emission is

$$\tau_{gw} = 1.8 \left( \frac{M_\odot}{M} \right) \left( \frac{P_{ms}^4}{R^2} \right) s \quad (17)$$

where again the stellar mass is in solar units, the radius is in km and the rotation period  $P$  is in milliseconds.

In a first approximation, the fraction of the mechanical energy which will be dissipated under the form of GWs is

$$f_g = \frac{1}{(1 + \tau_{gw}/\tau_d)}. \quad (18)$$

Notice that the damping time-scale by GW emission depends strongly on the rotation period. Therefore, one should expect that slow rotators will dissipate mostly of the mechanical energy into heat. In table 1 is shown for each star model the expected frequency of the fundamental mode (corrected for the gravitational redshift), the critical rotation period (in ms) for having  $f_g = 0.50$ , the GW damping for this critical period and the quality factor of the oscillation,  $Q = \pi \nu_0 \tau_{gw}$ .

Considering now a strongly magnetized neutron star with  $B \sim 10^{18} G$ , we detect an increasing in the gravitational mass of a star composed by pure hadronic matter. However, the gravitational mass of hybrid stars decrease for the case of increasing magnetic field and the explanation is quite simple: once the hybrid star has lower gravitational mass than the pure hadronic one, due to the presence of a softer quark matter in its inner shells and, the phase transition from hadron to quark matter occurs at lower densities with higher magnetic fields, the highly magnetized hybrid star will have a more important quark-gluon plasma core and a lower mass. This fact will represent a larger energy released during the phase transition and gravitational wave emission which could be detected from larger distances.

Table 1. Oscillation parameters for  $B=0$ : the damping time-scale  $\tau_{gw}$  is given for the critical period; maximum distances for VIRGO (V) and LIGO II (L) are in Mpc, and the LIGO II result for  $B=10^{18}G$ .

| $\nu_0$<br>(kHz) | $P_{crit}$<br>(ms) | $\tau_{gw}$<br>(ms) | Q<br>- | $D_{max}$<br>(VIRGO) | $D_{max}$<br>(LIGO II) | $D_{max}$<br>$B = 10^{18}G$ |
|------------------|--------------------|---------------------|--------|----------------------|------------------------|-----------------------------|
| 1.62             | 1.64               | 87.0                | 442    | 4.9                  | 10.2                   | 11.5                        |
| 1.83             | 1.25               | 27.0                | 155    | 6.4                  | 13.5                   | 15.28                       |
| 2.06             | 1.13               | 17.0                | 110    | 6.0                  | 12.8                   | 14.48                       |
| 2.32             | 1.06               | 11.5                | 84     | 5.1                  | 11.1                   | 12.56                       |
| 2.72             | 1.00               | 8.4                 | 72     | 3.6                  | 5.7                    | 6.45                        |

After filtering the signal, the expected signal-to-noise ratio is

$$(S/N)^2 = 4 \int_0^\infty \frac{|\tilde{h}(\nu)|}{S_n(\nu)} d\nu \quad (19)$$

where  $\tilde{h}(\nu)$  is the Fourier transform of the signal and  $S_n(\nu)$  is the noise power spectrum of the detector. Performing the required calculations, the S/N ratio can be written as

$$(S/N)^2 = \frac{4}{5} h_0^2 \left( \frac{\tau_{gw}}{S_n(\nu_{gw})} \right) \frac{Q^2}{1 + 4Q^2}. \quad (20)$$

In the equation above, the angle average on the beam factors of the detector were already performed.

From Eqs.(12) and (18), once the energy and the S/N ratio are fixed, one can estimate the maximum distance  $D_{max}$  to the source probed by the detector. In the last two columns of table 1 are given distances  $D_{max}$  derived for a signal-to-noise ratio  $S/N = 2.0$  and the sensitivity curve of the laser beam interferometers VIRGO and LIGO II. In both cases, it was assumed that neutron stars underwent the transition having a rotation period equal to the critical value.

We emphasize again that our calculations are based on the assumption that the deconfinement transition occurs in a dynamical time-scale<sup>24</sup>. In the scenario developed in Ref.<sup>10</sup>, a mixed quark-hadron phase appears and the complete deconfinement of the core occurs according to a sequence of quasi-equilibrium states. The star contracts slowly, decreasing its inertia moment and increasing its angular velocity until the final state be reached<sup>10</sup> in a time-scale of the order of  $10^5$  yr. Clearly, in this scenario no gravitational waves will

be emitted and this could be a possibility to discriminate both evolutionary paths.

## 8 Additional Effects

Additional effects and/or scenarios may improve, or not, the detection of gravitational waves from compact stars. An important aspect is related to the color super-conducting phase. As, in principle, this new phase would turn the equation of state even softer, enlarging the energy release during the astrophysical phase transition, we decided to analyze such a phase.

The super-conducting quark phase may be described by the thermodynamical potential<sup>25</sup>

$$\Omega_{CFL} = \Omega_{Free} - \frac{3}{\pi^2} \Delta^2 \mu^2 + B. \quad (21)$$

The resulting equation of state was evaluated and the TOV equations lead to a smaller radius star, as expected, but also to a less massive star, both for the gravitational and for the baryonic masses. This additional results do not change significantly the properties of gravitational wave emission as we have previously expected; however, we still expect an improved understanding about high-density matter properties to better describe such a phase.

The conversion from a neutron star to a strange star, instead of a hybrid star, is a more catastrophic event and may release much more energy, being detectable from longer distances. This kind of transition was studied by Bombaci<sup>18</sup>, in order to describe the emission of  $\gamma$ -ray bursts. Applying our results to describe the emission of gravitational waves we got the results shown in table 2, which leads to one of the most promising gravitational wave generators.

Table 2. Properties of a NS $\rightarrow$ SS conversion and the maximum distances for VIRGO (V) and LIGO II (L) are in Mpc

| $M_{bar}$ | $M_{SS}$ | $R_{SS}$ | $D_{max}^{Virgo}$ | $D_{max}^{Ligo}$ |
|-----------|----------|----------|-------------------|------------------|
| 1.0749    | 0.6445   | 8.40     | 15.47             | 34.63            |
| 1.3202    | 0.7804   | 8.87     | 20.01             | 44.79            |
| 1.5724    | 0.9241   | 9.30     | 24.27             | 54.33            |
| 1.8342    | 1.0727   | 9.68     | 28.20             | 63.13            |
| 2.1045    | 1.2210   | 9.98     | 32.07             | 71.79            |

## 9 Conclusions

Summarizing, in the framework of a nuclear many-body theory and the MIT bag model, the phase transition from hadron to quark matter was described by considering screening effects and the equation of state was determined. We applied the resulting EoS to the TOV equations also considering the effects of an intense magnetic field. The results obtained are in good agreement with previous results obtained by many authors. As a tool for gravitational wave emission, we considered the mechanism described in Ref.<sup>7</sup>, where a phase transition occurs inside a compact star and releases energy. According to the results, such an event would be detected as far as 13 Mpc without considering magnetic fields and 15 Mpc for compact star with  $B=10^{18}$ G. Considering a NS $\rightarrow$ SS transition, we obtained a much larger distance of up to 71 Mpc.

## 10 Acknowledgements

The author would like to thank Profs. J. A. de Freitas Pacheco, M. Dillig, C. A. Z. Vasconcellos and Dr. A. R. Taurines for the stimulating discussions on the topics covered in this contribution and the workshop organizers for this opportunity.

## References

1. B.D. Serot, J.D. Walecka, *Adv. Nucl. Phys.* 16:1,327,1986; *Int. J. Mod. Phys.* E6:515-631, 1997.
2. A. Chodos, R. L. Jaffe, K. Johnson, C. B. Thorn and V. F. Weisskopf, *Phys. Rev.* **D9**, 3471 (1974).
3. J. Boguta and A. Bodmer, *Nucl. Phys.* **A292**, 413 (1977).
4. J. Zimanyi and S. A. Moszkowski, *Phys. Rev.* **C42**, 1416 (1990).
5. A.R. Taurines, C.A.Z. Vasconcellos, M. Malheiro, M. Chiapparini, *Phys. Rev.* C63:065801, 2001.
6. G.F. Marranghello, C.A.Z. Vasconcellos, J.A. de Freitas Pacheco, M. Dillig, *Int.J.Mod.Phys.* E11:83-104, 2002.
7. G. F. Marranghello, C. A. Z. Vasconcellos and J. A. de Freitas Pacheco, *Phys. Rev.* **D66**, 064027 (2002).
8. N. K. Glendenning, F. Weber and S. A. Moszkowski, *Phys. Rev.* **C45**, 844 (1992).
9. H. Heiselberg and M. Hjorth-Jensen, nucl-th/9902033.
10. N. K. Glendenning, *Phys. Rev.* **D46**, 1274 (1992).
11. D. Lai and S. Shapiro, *ApJ.* **442**, 259 (1995).

12. A. Broderick, M. Prakash and J. M. Lattimer, astro-ph/0001537.
13. A. Broderick, M. Prakash and J. M. Lattimer, Phys. Lett. **B**, 531 (2002) 167..
14. D. Bandyopadhyay, S. Chakrabarty and S. Pal, astro-ph/9703066.
15. R. C. Tolman, Phys. Rev. **55**, 364 (1939).
16. J. R. Oppenheimer and G. M. Volkoff, Phys. Rev. **55**, 374 (1939).
17. V. Olinto, Phys. Lett. **B**, 192 (1987) 71.
18. I. Bombaci, Lect. Notes in Phys. **578:Physics of Neutron Star Interiors**, edited by D. Blaschke, N. K. Glendenning, A. Sedrakian (Springer-Verlag, 2001).
19. J. A. de Freitas Pacheco, Proceedings of the VI International Workshop on Relativistic Aspects of Nuclear Physics, ed. T.Kodama et al., World Scientific, 2001, p.158
20. P.K. Sahu and G.F. Burgio and M. Baldo, ApJ **566**, L89 (2002).
21. P. Haensel and J.L. Zdunik and R. Schaeffer, A&A **217**, 137 (1989).
22. G. Miniutti and J. A. Pons and E. Berti and L. Gualtieri and V.Ferrari, astro-ph/0206142.
23. Qing-de Wang and Tan Lu, Chin.Astr.Astrophys. **9**, 159 (1984).
24. P. Haensel and M. Prózyński, ApJ **258**, 306 (1982).
25. G. Lugones and J. E. Horvath, Phys. Rev. **66**, 074017 (2002).